RSC Advances

ROYAL SOCIETY OF CHEMISTRY

www.rsc.org/advances

Removal and recycling of ppm level methylene blue from aqueous solution with graphene oxide

Saijie Song[a,b], *Yufei Ma*[*a], *He Shen*[a], *Mengxin Zhang*[a,b], *and Zhijun Zhang*[*a]

[a]Key Laboratory of Nano-Bio Interface, Division of Nanobiomedicine, Suzhou Institute of Nano-Tech and Nano-Bionics, Chinese Academy of Sciences, Suzhou 215123, China

[b]University of Chinese Academy of Sciences, 19(A) Yuquan Road, Beijing, 100039, China

ABSTRACT

Dye-containing wastewater is one of major issues in the water contamination, and its treatment remains a serious problem due to low concentrations of dyes in polluted natural water and high cost for its purification. Herein, we report the application of graphene oxides (GO) in decontamination of ppm level of methylene blue (MB) in aqueous solution. During the dye removal process, GO adsorbs MB molecules via strong interactions including π-π stacking and electrostatic attraction, and facilitates the precipitation of GO/MB complexes, which can be readily removed from the solution. The adsorption progress follows the Langmuir isotherm model and the pseudo-second-order kinetic model. The thermodynamic parameters indicate that the adsorption progress is a spontaneous progress. By using our strategy, a dye removal rate as high as 95% has been achieved with a final dye concentration of only 0.25 ppm. In addition, 82% of dye can be recycled through ethanol extraction from the collected GO/MB complexes. All the results demonstrate that GO nanosheets can effectively remove and recover ppm level of cationic dye pollutants represented as MB, showing promising application of GO in ultra-low concentration dye containing wastewater treatment.

KEYWORDS: graphene oxide; methylene blue; adsorption; ppm level; recycle

INTRODUCTION

The development of human society has caused huge disaster to the environment,[1] which poses a threat to human health. Among a variety of environmental problems, water pollution is one of the most severe global matters,[2] and has caused great restriction to sustainable development of human society with widespread and severe damage. Dyes have become the main pollutant in all kinds of water pollution, due to their wide applications in various fields, such as textile, paper, rubber, plastic, leather, cosmetic, pharmaceutical and food industries.[3, 4] About 5-15% of dyes are lost during industrial usage and released into open waters after simple pretreatment, resulting in huge waste of resources and inestimable disaster to our environment.[5, 6] And even worse, most of dye pollutants are toxic and even carcinogenic and teratogenic to humankind and animals, with high solubility in water and poor biodegradability.[7, 8] Therefore, it is important to treat dye-contaminated wastewater and recycle the lost dyes.

Among various technologies of removing dye pollutants (adsorption,[9, 10] biological methods,[4, 11] chemical oxidation,[12, 13] photocatalytic degradation[14]) from wastewater, adsorption is one of the most effective and favorable methods due to its high removal efficiency, low processing cost, and simple operation procedure.[15-17] The materials developed to remove dye from wastewater include activated carbon,[18] montmorillonite clay,[19] biosorbents,[20, 45] and a variety of nanomaterials especially carbon-based nanomaterials.[3, 21] Recently, graphene, a two-dimensional nanomaterials consisting of hexagonal array of sp^2-bonded carbon atoms, has attracted considerable attention in the field of environmental science for its super large surface area (2630 m^2/g) and flat structure.[22, 23] As one of the most important derivatives of graphene, graphene oxide (GO) has been applied to remove cationic dye pollutants in solution, because its huge negatively charged surface could adsorb aromatic dye molecules via π-π stacking and electrostatic interactions.[24, 25] For example, Yang et al.[26] reported that GO can be directly utilized to remove methylene blue (MB) from initial concentration

of 250 mg/L to 1.4 mg/L, owing to its excellent adsorption performance; Liu et al.[27] demonstrated that a three-dimensional (3D) graphene oxide sponge could efficiently remove dyes such as MB and MV (methyl violet); Zhang et al.[28] showed that GO prepared via a modified Hummer's method could adsorb MB very quickly but hardly release the dyes; Yan et al.[21] recently compared the MB adsorption ability of a series of GO with different oxidation degrees (OD), and suggested that OD increase could induce exponentially improved loading of GO to dyes.

In many previous reports about using GO for dye removal form wastewater, the initial dye concentrations were often at hundreds of ppm level,[21,26,27,34] and the dye concentrations generally remain at several ppm after adsorption process.[21,27,34] Indeed, some dye-removal strategies through advanced oxidation process and photocatalytic degradation, which succeed with ppm level dye wastewater in some experiments,[29, 30] require a high dosage of catalytic materials and waste the dyes. Therefore, it is still a big challenge to efficiently remove low concentration pollutants from natural water system, especially via simple and inexpensive approaches.

We have reported in our previous work that GO showed excellent biocompatibility and adsorbing capability to aromatic molecules, such as doxorubicin and camptothecin (both are widely used anticancer drugs in clinic), and tetracycline (an antibiotic found as a contaminant in the environment).[31, 32] Herein, we demonstrate the successful application of GO for treatment of several ppm level of MB, and probe the effects of the initial concentration of MB, the dosage of GO, pH value, ionic strength, and temperature on the removal efficiency. To further comprehend the adsorption progress, we studied the isotherm via fitting the experimental data to the Langmuir, Freundlish, Temkin, Redlich-Peterson, Sips, and Dubinin-Radushkevich models and kinetic via fitting the experimental data to the pseudo-first-order, pseudo-second-order and Elovich equation model, as well as calculated the thermodynamic parameters (ΔG^0, ΔH^0 and ΔS^0) of the adsorption progress. Finally,

we explored the use of GO to the removal of ppm level MB in natural water and the recycling of MB from the GO sheets.

EXPERIMENTAL SECTION

Materials. GO was prepared by a modified Hummers method identical to our previous reports.[31,33] An aqueous solution of GO (5 mg/mL) was made with D.I. water as GO stock solution for use. MB (Sigma) was dissolved in D.I. water, or natural water to prepare simulated wastewater (250 mg/mL). The natural water was obtained from the stream in front of SINANO, CAS, and was filtered through filter paper (fast filtering speed, Sinopharm Chemical Reagent) to avoid UV-vis absorbance interference from impurities such as large soil particles.

Instrumentation. Atomic force microscope (AFM) was a Vecco Dimension 3100 atomic force microscope. Fourier transform infrared spectra were conducted within the 4000~400 cm^{-1} wavenumber range with the KBr pellet technique by a Thermo Nicolet 6700 FTIR spectrometer. UV-Vis spectra were collected in the 200~800 nm wavelength range with a Perkin-Elmer Lambda 25 spectrophotometer.

Adsorption of MB by GO. MB stock solution (250 mg/L) was diluted with D.I. water or natural water to the required concentrations before use. GO mixed with MB was stirred at 300 rpm for 20 min, and then kept for 4 h at room temperature to allow the precipitation of GO/MB. The schematic of the adsorption of MB onto GO is showed in Fig 1.

After the removal experiment, the liquid supernatant was separated from the remained precipitate by centrifuging at 12,000 rpm for 15 min. The residual concentration of MB in the solution was determined via a maximal absorbance at λ_{max}=664 nm.
The removal rate (1) of MB and the adsorption capacity (2) of GO was assessed by the following equations:

$$R_e = \frac{C_0 - C_e}{C_e} \times 100 \quad (1)$$

$$q_t = \frac{C_0 - C_t}{W} \times V \quad (2)$$

where R_e is the percentage of dye removal (%); q_e is the amount of dye adsorbed on adsorbent at equilibrium (mg/g); C_0 (mg/L) is the initial concentration of dye (mg/L), C_e is the concentration of dye at equilibrium (mg/L); C_t is the concentration of dye at different periods of times (mg/L); V is the volume of solution (L); W is the mass of absorbent (g).

Kinetic study for the MB adsorption. The adsorption experiments were conducted following the above-mentioned procedure, while the initial concentrations of MB and GO were kept at 5 and 15 ppm, respectively. At certain time point (10, 20, 30, 40, 60, 90, 120, 150, and 180 min), 0.1 mL out of the 50 mL solution was taken and then processed with centrifugation to measure the concentration of free MB in the solution by UV.

Three kinetic models, pseudo-first-order (3), pseudo-second-order (4), Elovich equation (5) and intraparticle diffusion (6) models[35] are employed to investigate the adsorption mechanism of dye onto adsorbent.

$$\ln(q_e - q_t) = \ln q_e - k_1 t \quad (3)$$

where q_t is the amount of dye adsorbed on adsorbent at different tim (mg/g); k_1 is the adsorption rate constant (min^{-1}).

$$\frac{t}{q_t} = \frac{1}{k_2 q_e^2} + \frac{1}{q_e} t \quad (4)$$

where k_2 is the pseudo-second-order rate constant (g/mg min)

$$q_t = \frac{1}{\beta}\ln(\alpha\beta) + \frac{1}{\beta}\ln t \quad (5)$$

where α is the initial adsorption rate (mg/g min) and β is the desorption constant (g/mg).

$$q_t = k_i t^{1/2} + l \quad (6)$$

where k_i is the intraparticle diffusion constant and l is the effect of boundary layer thickness.

Isotherm models for MB adsorption. The adsorption experiments were conducted following the above-mentioned procedure, while the initial concentrations of and GO were kept at 15 ppm, and MB in the range of 5-30 ppm. The adsorption isotherms of the adsorption process are utilized to inspect the performance of the adsorption process. Two most used isotherm models, the Freundlich (7), Langmuir (8), Temkin (9), Redlich-Peterson (10), Sips (11), and Dubinin-Radushkevich (12) models,[35] are employed to fit the experiment data as follows:

$$\ln q_e = ln\, K_F + \frac{1}{n} ln\, C_e \quad (7)$$

where K_F (L/g) is the Freundlich constants related to adsorption capacity and n is a constant related to the adsorption intensity.

$$\frac{C_e}{q_e} = \frac{C_e}{q_m} + \frac{1}{q_m K_L} \quad (8)$$

where q_m is the maximum adsorption capacity of GO for MB (mg/g); K_L is the Langmuir constant and is related to the free energy of adsorbent (L/mg).

$$q_e = \frac{RT}{b} ln(K_T C_e) \quad (9)$$

where K_T is the Temkin isotherm equilibrium binding constant (L/g); b is the Temkin isotherm constant.

$$q_e = \frac{K_{RP} C_e}{1+\alpha_{RP} C_e^{\beta}} \quad (10)$$

where K_{RP} is the Redlich-Peterson constant (L/g); α_{RP} is a constant $((L/g)^{\beta})$; β is an exponent varying between 0 and 1.

$$q_e = \frac{q_m K_S C_e^{1/n}}{1+K_S C_e^{1/n}} \quad (11)$$

where K_S is the Sips constant $((L/mg)^n)$; n is the Sips model exponent. For n=1, eqn (11) reduces to Langmuir isotherm (eqn (8)). Alternatively, for low equilibrium concentration, close to 0, the Sips isotherm reduces to the Freundlich isotherm (eqn (7))。

$$\ln q_e = \ln q_m - \beta \varepsilon^2 \quad (12)$$

where β is the activity coefficient related to mean sorption energy; ε is the Polanyi potential, which is equal to

$$\varepsilon = \mathrm{RTln}(1 + \frac{1}{C_e}) \quad (13)$$

where R is the gas constant (J/mol K); T is the temperature (K).

Thermodynamics study. The adsorption experiments were conducted following the above-mentioned procedure, while the initial concentrations of MB and GO were kept at 5 and 15 ppm, respectively. Various temperatures (298-343 K with intervals of 15 K) were applied during the adsorption process.

The thermodynamic parameters of the adsorption progress are calculated via the following equations: [34]

$$\Delta G^0 = -RT\ ln\ K \quad (14)$$

$$\mathrm{K} = \frac{q_e}{C_e} \quad (15)$$

$$\ln K = \frac{\Delta S^0}{R} - \frac{\Delta H^0}{RT} \quad (16)$$

where ΔG^0 is the free energy change; ΔH^0 is the enthalpy change; ΔS^0 is the entropy change; K is the equilibrium constant, R is the universal gas constant (J/mol K); T is the temperature (K).

The adsorption of other dyes on GO. The process was similar to the MB adsorption for the experiments of neutral red (NR), Malachite Green (MG), and rhodamine B (RhB), except for the initial concentrations of MG and RhB, which only work at high dye concentrations.

Recycle of MB. The flocculent compound precipitated out from solution was collected by centrifuging at 12,000 rpm for 15 min. Then ethanol and NaCl was applied to dissolve MB, and the solution was separated from GO via centrifugation (12,000 rpm, 10 min each time). The procedure was repeated for several times until ethanol solution appeared colorless. The collected ethanol solution of MB was characterized with UV-vis spectra for the estimation of MB concentration and recycling efficiency. After recycling process, the precipitate was washed with D.I.

water to remove NaCl for further dye removal and recycling. The adsorption and recycling processes were repeated for 5 times.

RESULTS AND DISCUSSION

Characterization of GO. GO was prepared by oxidation of graphite with the modified Hummers method as our previous report.[31,33] Thus-obtained GO sample has good dispersity in water, forming stable yellow-brown solution. As shown in the UV-Vis spectrum of GO (Fig 2a), the maximum absorption peak of GO appears at 231 nm and its absorption from 600~800 nm is nearly zero, bringing no interference for quantification of MB. The FTIR spectrum of GO (Fig 2b) indicates the existence of –OH (3420cm^{-1}), C=O (1730 cm^{-1}), C=C (1625 cm^{-1}), and C-O (1065 cm^{-1}) groups, respectively. AFM image (Fig 2c) shows that the thickness of GO is about 1-2 nm, which corresponds to 1-2 layer graphene. Zeta potentials (Fig 2d) of GO were measured in D.I. water at pH 3~11 (adjusted by 0.1 M HCl and 0.1 M NaOH) on a Malvern Zetasizer Nano ZS90. The highly negative zeta potentials of GO indicates that GO is stable and exhibits the ability to the adsorption of cationic dye in a wide pH range. All the data are in accordance with literature. [35,36]

Initial concentration of MB and the dosage of GO. To efficiently gather and remove ppm level of cationic dye pollution such as MB, GO was employed as the very adsorbent. First, we applied a series of initial concentrations for MB or GO to determine the ratio of GO/MB at which an optimal dye removal performance was achieved. As shown in Fig 3a & 3b, a removal efficiency as high as 95% can be achieved when GO: MB was 3:1. It's reasonable that the removal rate drops when GO/MB < 3 due to deficient GO absorbents; under the circumstances when GO/MB > 3, the decreased removal may result from the good dispersity of GO in water, because only little precipitate was observed (Fig. S1).

During the dye removal process, a large amount of floccule occurred very quickly (<1 min) after mixing MB and GO (Fig. S1 & S2), and can be easily removed through centrifugation. Fig. 3c shows the UV-Vis spectra of the solutions after floccule removal. When the ratio of GO:MB is 3:1, there is little absorption both in the visible-light and UV region, suggesting almost complete removal of GO and MB; deficient GO (GO:MB=1:1) presents identical absorption peaks resembling MB in the UV-Vis spectrum; if the amount of GO increases to as much as 5 times of MB, most of MB molecules stay in the solution because GO is soluble in water, while the absorption peaks greatly shift to the shorter wavelength (a new peak at 583 nm) and became weak and broad, indicating strong π-π stacking and electrostatic interaction between GO and MB molecules.[37]

In order to deeply understand the interactions between GO and MB, we conducted FTIR analysis (Fig. 3d & S3) on the floccule collected during the dye removal procedure. For the sample with GO:MB=3:1, the stretching vibration of C=O at 1730 cm^{-1} shows similar pattern to that of GO; the aromatic skeletal C=C stretching vibrations of graphitic domains at 1625 cm^{-1} disappears, and the skeletal stretching of aromatic rings at 1600 and 1444 cm^{-1} shifts by 4 cm^{-1} to lower wavenumbers, suggesting π-π stacking between the aromatic structures of GO and MB; the stretching vibration of tertiary amines belonging to MB at 1355 and 1344 cm^{-1} shifted to lower wavenumbers, and the intensity ratio of these two peaks significantly changed compared to pristine MB. All these changes in FTIR spectra suggest the strong π-π stacking between GO and MB, as has been mentioned in previous reports.[38] In the spectrum of the sample with GO:MB=24:1, in which all the dye molecules attach to GO surfaces, it all verifies the assumption of π-π stacking that the distinctive shifts of the vibration at 1600, 1444, and 1338 cm^{-1}, as well as the different peak ratio of 1355 and 1338 cm^{-1}. Therefore, it is proposed that the removal of the dye pollutant by GO was mainly due to strong π-π interactions, which leads to GO's adsorption of MB molecules and then the aggregation of GO/MB complexes.

Effect of the solution pH. The solution pH can change the net charge of the adsorbent and adsorbate, and subsequently influence the interaction between them.[39] Fig 4a shows the effect of the solution pH on MB removal efficiency by GO with the initial pH ranging from 3.0 to 11.0. In the pH range from 5.0 to 9.0, the removal rate of MB remained around 95% (final $C_{MB} \approx 0.25$ ppm), while the removal efficiency declined to 85% at pH 3.0. Interestingly, a dramatic drop of MB removal efficiency to 0% at pH 11.0 was observed, since no floccule was formed at all. Based on the results that the solution color turned to bluish violet at pH 11.0 (Fig. 4b & S4) with an absorption peak ~575 nm, we assume the existence of GO/MB complexes in the solution, which was then verified by IR spectral measurement (two peaks appears at 1338, 1444 cm^{-1}) (Fig. 4c & S5). The aqueous stability of GO/MB complexes at low concentrations is likely due to the deprotonation of the carboxyl groups on GO and the consequent electrostatic repulsion.[40,41] In addition, the adsorption capacity of GO may increase a little bit at high pH value.[28]

It is well known that GO possesses abundant oxygen-containing functional groups, such as hydroxyl and carboxyl groups,[24, 25, 42] allowing GO with a negatively charged surface. As a typical cationic dye, MB molecules present positive charge in aqueous solution, making it being easily adsorbed by GO. At low pH (such as pH=3.0), the carboxyl groups on GO's surfaces stay protonated, minimizing the negative charges on GO surface. In this case, the electrostatic interaction between GO and MB is prohibited to some extent, so less MB molecules are adsorbed on GO's surface. This electrostatic interaction playing a role in the formation of GO/MB complexes agrees other observations.[28] Besides, we only observed small variation of MB removal rate in the pH range of 3.0-9.0. As this phenomenon may suggests, the electrostatic attraction represents a small portion of the interaction between GO and MB, while the π-π stacking dominate the adsorption process.

Effect of ionic strength. Other than various pollutants, industrial wastewater often contains a large amount of salts, such as NaCl. The existence of ions has significant influence on the removal efficiency of pollutants, [43,44] through affecting the interaction between the adsorbent and adsorbate. As showed in Fig 5, a certain amount of NaCl (<5 mM) improves the removal rate. In addition, the solution with 5 mM NaCl turned clear in 2 hours with a lot of floccule regardless of stirring, while the solution without NaCl showed no aggregates at all, even after two days (Fig. S6). Compared to other reports, the role of NaCl in efficient dye removal seems crucial for our GO sample and the aggregation of GO/MB. We suspect that the possibility of GO for dye removal at ppm levels results from the excellent aqueous stability of our GO sample, which enables GO adsorbing MB molecules to reach its maximum before the precipitation of GO/MB. Besides, the fact that NaCl facilitates MB removal in our experiments may be due to the salting-out effect by decreasing the solubility of GO connected with MB. However, the adsorption rate decreased gradually when the concentration of NaCl was above 5 mM. As the amount of NaCl increases, the greatly enhanced ionic strength contributes to a stable ion solution and prevents GO/MB from being separated from solution. [43,44] It should be noted that the concentrations of the dye and GO in our study were within ppm level (10^{-6} M) and are far lower than that of NaCl.

Effect of temperature. Temperature has significant influence to the removal efficiency of MB by GO via interfering molecular diffusion and the interaction between adsorbate and adsorbent.[28] Fig 6 shows the effect of temperature on the dye removal rate. With the increase of temperature, the removal rate decreases a lot, indicating that the adsorption progress is an exothermic progress.[28, 35]

Adsorption kinetics analysis. Kinetics analysis was studied to estimate the effectiveness of GO and inspect the mechanism of MB adsorbed onto GO. Fig 7a presents the MB amount absorbed onto GO as function of time. For the adsorption of

MB molecular onto the external surface of GO particles, the adsorption progress rapidly carries out in the first 10 min, and reaches the maximum adsorption capability in about 90 min. To simulate the adsorption progress, three common kinetic models, including the pseudo-first-order, pseudo-second-order and Elovich equation, were employed. Fig. 7b and Figure S7 & S8 shows the linear plots of t/q_t vs. t, ln (q_e-q_t) vs. t, and q_t vs. ln t, respectively. All the non-linear fitting results are calculated and listed in Table 1. The determination coefficients R^2 of the pseudo-first-order and Elovich model are lower than that of pseudo-second-order rate model, indicating that the adsorption kinetic model of MB onto GO fits the pseudo-second-order model well. This conclusion agrees well with previous reports.[21, 34, 45]

To further understand the dye adsorption progress, the intraparticle diffusion model was employed to analyze the diffusion mechanism of MB. Fig 8 shows the plot of q_t vs. $t^{1/2}$, and the values of intraparticle diffusion rate constant (k_i) and the effect of boundary layer thickness (l) are listed in Table 1. The plot in Fig 8 is not linear during the whole time range, indicating that the key step determining MB adsorption onto GO is not the intraparticle diffusion, in which progress the dye molecules diffuse from the surface into the adsorbent interior. The boundary layer diffusion is also significant for the adsorption process in our case.[35]

Isothermal adsorption equilibrium study. To further comprehend the adsorption progress, we employ the Freundlich, Langmuir, Temkin, Redlich-Peterson, Sips, and Dubinin-Radushkevich isotherm models to fit the experimental data. The adsorption isotherm plots for MB adsorbed on GO are presented in Fig 9 and the simulation results are listed in Table 2. The results show that the correlation coefficient (R^2) of the linear for Langmuir model is higher than that of other isotherm models. As the good fit with Langmuir model indicates, the adsorption of MB by GO takes place in a monolayer adsorption manner, and of little roughness is the GO surface. Similar conclusions has also been revealed in previous reports.[21, 34, 45] In addition, the maximum adsorption capacity of GO calculated from Langmuir isotherm is 909.1

mg/g, which is higher than the values in previous reports[21,26,27,34,45] (Table 3, typically 200-700 mg/g) and indicates that GO is a promising adsorbent for MB removal.

Thermodynamics analysis. Owing to the important effect of temperature in adsorption progress, we calculated the thermodynamics parameters of MB adsorbed onto GO. From the plot of ln K vs. 1/T (Fig 10), the free energy change ΔG^0 at various temperature is obtained, as well as the enthalpy ΔH^0 (-22.91 kJ/mol) and entropy ΔS^0 (28.88 J/mol K) (Table 4). The negative values of ΔG^0 indicate that the adsorption progress of MB onto GO is thermodynamically possible and spontaneous. The negative value of ΔH^0 indicates that the progress is exothermic. The negative value of ΔS^0 indicates the reduced randomness at the solid-solution interface of MB adsorbed onto GO.

Adsorption of other dyes onto GO. To verify the applicability of GO as a promising adsorbent for adsorbing and removing cationic dyes, we employed neutral red (NR, Fig S12a), a dye with similar molecular structure to MB (Fig S12b), as a representative to inspect the adsorption capability of GO. We found that the adsorption progress was easy to take place and a mass of precipitate occurred with vigorous stirring. A removal rate of 92.93% was obtained under the condition of 11.2 mg/L GO and 7.5 mg/L NR (Fig S9). The adsorption progress fits Langmuir isotherm model (Fig S10, R^2=0.9937), and the calculated q_m is 714.3 mg/g. Similar to MB, the adsorption kinetics of NR adsorbed onto GO also follows the pseudo-second-order (Fig S11, R^2=0.996). In addition to MB and NR, two other cationic dyes, malachite green (MG, Fig S12c) and rhodamine B (Rh B, Fig S12d), were tested with GO. A mass of precipitate occurred at hundreds of ppm for dyes (Table S1), but not at ppm levels for MG and Rh B. However, the calculated q_m for MG and Rh B at high concentrations are 909.1 and 833.3 mg/g, respectively, strongly indicating that GO is a promising adsorbent for the dye wastewater treatment.

Remove MB from natural water. Natural water contains many kinds of impurities, such as suspended solids, inorganic salts, organic compounds, and microorganism, which would influence the removal effect of MB by GO. Therefore, a simulated wastewater was prepared by dissolving MB in a natural water sample from a stream in front of SINANO, CAS, China. Fig 11a suggests that a ratio of 5:1 for GO: MB can lead to the best MB removal efficiency of as high as 88% in natural water. The requirement of more GO in natural water than D.I. water may be due to the presence of many impurities in the natural water (Fig. S13). As shown in Fig 10b, the UV absorbance of the solution after the dye removal process is weaker than that of natural water only, indicating the removal of the impurities from natural water by GO.

Recycling of MB. Recycling of dyes from wastewater not only solves an environmental problem, but also saves reusable resources and reduces industrial cost. Hence, we examined the recycling rate of MB and GO from the GO/MB complexes. It was easy to collect the GO/MB conjugates, which is in the form of a large amount of floccule. MB was then recycled from the GO/MB residues though ethanol extraction in the presence of NaCl. The recycling rate was as high as 82%, which is more than 2 times of a recycling rate (37%) with GO in previous reports.[28] In addition, we reused the recovered GO residues for further MB adsorption and recycling, and found that the recycling rate kept as high as more than 60%, even after 5 time of reuse of GO. The recycling rate of MB decreased upon the increase of usage times of GO (Fig.12), which may be due to the small loss of GO during the separation procedure of GO/MB complexes. The procedure of dye collection in the solution with ppm level of MB is simple and inexpensive, showing a promising approach in purification of low concentration wastewater and recycle of pollutant simultaneously.

In conclusion, our study clearly shows the feasibility of using GO for the removal of ppm level cationic dye through simple adsorption, with a high removal efficiency (95%) and a low final dye concentration (0.25 ppm). Our experiment indicated that a

certain ratio of GO to MB (3:1) resulted in the optimal dye removal effect. Other than the amount of GO, the removal efficiency could be slightly influenced by pH and ionic strength. We next studied the kinetics and thermodynamics of the MB adsorption on GO, and found that the adsorption followed Langmuir adsorption model pseudo-second-order. In addition, we used natural water dissolving 5 ppm of MB to simulate the wastewater, and found that the impurities in the natural water could be adsorbed by GO, and thus caused increase in the amount of GO and decrease in the dye removal efficiency to 88%. At last, we recovered 82% of MB through ethanol extraction from the dye wastewater, demonstrating an economic way to treat water pollutions. Our findings may provide an efficient way to removal and recycling of very low concentration dye pollutants from wastewater.

ASSOCIATED CONTENT

Supporting Information

Additional Figure S1 – S13 and Table S1. This material is available free of charge via the Internet at http://pubs.rsc.org/.

AUTHOR INFORMATION

*** Corresponding Authors.**

Fax: 86-512-62603079; Tel: 86-512-62872556;

E-mails: yfma2012@sinano.ac.cn (Y. Ma), zjzhang2007@sinano.ac.cn (Z. Zhang).

Author Contributions

The manuscript was written through contributions of all authors. All authors have given approval to the final version of the manuscript.

ACKNOWLEDGEMENTS

We acknowledge financial support of this work from National Natural Science Foundation of China (No. 51361130033) and the Ministry of Science and Technology of China (No. 2014CB965003).

REFERENCES

1. Schipper, L.; Pelling, M. *Disasters* **2006,** *30*, (1), 19-38.
2. Schwarzenbach, R. P.; Egli, T.; Hofstetter, T. B.; Von Gunten, U.; Wehrli, B. *Annu. Rev. Environ. Resour.* **2010,** *35*, 109-136.
3. Gong, J.-L.; Wang, B.; Zeng, G.-M.; Yang, C.-P.; Niu, C.-G.; Niu, Q.-Y.; Zhou, W.-J.; Liang, Y. *J. hazard. mater.* **2009,** *164*, (2), 1517-1522.
4. Popli, S.; Patel, U. D. *Int. J. Environ. Sci. Te.* **2014**, 1-16.
5. Al-Ghouti, M.; Khraisheh, M.; Allen, S.; Ahmad, M. *J. Environ. Manage.* **2003,** *69*, (3), 229-238.
6. Rai, H. S.; Bhattacharyya, M. S.; Singh, J.; Bansal, T.; Vats, P.; Banerjee, U. *Crit. Rev. Env. Sci. Tec.* **2005,** *35*, (3), 219-238.
7. Carvalho, M.; Pereira, C.; Goncalves, I.; Pinheiro, H.; Santos, A.; Lopes, A.; Ferra, M. *Int. Biodeter. Biodegr.* **2008,** *62*, (2), 96-103.
8. Uddin, M. T.; Islam, M. A.; Mahmud, S.; Rukanuzzaman, M. *J. Hazard. Mater.* **2009,** *164*, (1), 53-60.
9. Crini, G. *Bioresour. technol.* **2006,** *97*, (9), 1061-1085.
10. Sharma, P.; Das, M. R. *J. Chem. Eng. Data.* **2012,** *58*, (1), 151-158.
11. An, H.; Qian, Y.; Gu, X.; Tang, W. Z. *Chemosphere* **1996,** *33*, (12), 2533-2542.
12. Szpyrkowicz, L.; Juzzolino, C.; Kaul, S. N. *Water Res.* **2001,** *35*, (9), 2129-2136.
13. Gogate, P. R.; Pandit, A. B. *Adv. Environ. Res.* **2004,** *8*, (3), 501-551.
14. Konstantinou, I. K.; Albanis, T. A. *Appl. Catal. B: Environ.* **2004,** *49*, (1), 1-14.
15. Zhou, L.; Gao, C.; Xu, W. *ACS appl. mater. inter.* **2010,** *2*, (5), 1483-1491.
16. Junyong, C.; Yongmei, H.; Yan, L.; Jiajia, G. *RSC Adv.* **2013,** *3*, (20), 7254-7258.
17. Sivakumar, P.; Palanisamy, P. *Int. J. ChemTech. Res.* **2009,** *1*, (3), 502-510.

18. Hameed, B.; Din, A. M.; Ahmad, A. *J. hazard. mater.***2007,** *141*, (3), 819-825.

19. Almeida, C.; Debacher, N.; Downs, A.; Cottet, L.; Mello, C. *J. colloid interface sci.* **2009,** *332*, (1), 46-53.

20. Han, R.; Zou, W.; Yu, W.; Cheng, S.; Wang, Y.; Shi, J. *J. hazard. mater.* **2007,** *141*, (1), 156-162.

21. Yan, H.; Tao, X.; Yang, Z.; Li, K.; Yang, H.; Li, A.; Cheng, R. *J. hazard. mater.* **2014,** *268*, 191-198.

22. Wang, S.; Sun, H.; Ang, H.-M.; Tadé, M. *Chem. Eng. J.* **2013,** *226*, 336-347.

23. Yang, Y.; Xie, Y.; Pang, L.; Li, M.; Song, X.; Wen, J.; Zhao, H. *Langmuir* **2013,** *29*, (34), 10727-10736.

24. Erickson, K.; Erni, R.; Lee, Z.; Alem, N.; Gannett, W.; Zettl, A. *Adv. Mater.* **2010,** *22*, (40), 4467-4472.

25. Marcano, D. C.; Kosynkin, D. V.; Berlin, J. M.; Sinitskii, A.; Sun, Z.; Slesarev, A.; Alemany, L. B.; Lu, W.; Tour, J. M. *ACS nano* **2010,** *4*, (8), 4806-4814.

26. Yang, S.-T.; Chen, S.; Chang, Y.; Cao, A.; Liu, Y.; Wang, H. *J. colloid interface sci.* **2011,** *359*, (1), 24-29.

27. Liu, F.; Chung, S.; Oh, G.; Seo, T. S. *ACS appl. mater. inter.* **2012,** *4*, (2), 922-927.

28. Zhang, W.; Zhou, C.; Zhou, W.; Lei, A.; Zhang, Q.; Wan, Q.; Zou, B. *B. environ. contam. tox.* **2011,** *87*, (1), 86-90.

29. Haldorai, Y.; Kim, B. K.; Jo, Y. L.; Shim, J. J. *Mater. Chem. Phys.* **2014,** *143*, (3), 1452-1461.

30. Lv, T.; Pan, L.; Liu, X.; Sun, Z. *Catal. Sci. Technol.* **2012,** *2*, (11), 2297-2301.

31. Zhang, L.; Xia, J.; Zhao, Q.; Liu, L.; Zhang, Z. *Small* **2010,** *6*, (4), 537-544.

32. Zhang, Y.; Chen, B.; Zhang, L.; Huang, J.; Chen, F.; Yang, Z.; Yao, J.; Zhang, Z. *Nanoscale* **2011,** *3*, (4), 1446-1450.

33. Hummers Jr, W. S.; Offeman, R. E. *J. Am. Chem. Soc.* **1958,** *80*, (6), 1339-1339.

34. Li, Y.; Du, Q.; Liu, T.; Peng, X.; Wang, J.; Sun, J.; Wang, Y.; Wu, S.; Wang, Z.; Xia, Y. *Chem. Eng. Res. Des.* **2013,** *91*, (2), 361-368.

35. Paşka, O. M.; Păcurariu, C.; Muntean, S. G. *RSC Adv.* **2014**, *4*, 62621.

36. Ai, L.; Jiang, J. *Chem. Eng. J.* **2012,** *192*, 156-163.

37. Jing, P.; Ji, W.; Yuan, X.; Ikezawa, M.; Zhang, L.; Li, H.; Zhao, J.; Masumoto, Y. *J. Phys. Chem. Lett.* **2013,** *4*, (17), 2919-2925.

518 38. Shi, H.; Li, W.; Zhong, L.; Xu, C. *Ind. Eng. Chem. Res.* **2014,** *53*, (3), 1108-1118.

519 39. Li, Y.; Zhang, P.; Du, Q.; Peng, X.; Liu, T.; Wang, Z.; Xia, Y.; Zhang, W.; Wang, K.; Zhu, H. *J.*

520 *colloid interface sci.* **2011,** *363*, (1), 348-354.

521 40. Pang, S.; Gao, Y.; Li, Y.; Liu, S.; Su, X. *Analyst* **2013,** *138*, (9), 2749-2754.

522 41. Ahn, H.; Kim, T.; Choi, H.; Yoon, C.; Um, K.; Nam, J.; Ahn, K. H.; Lee, K. *Carbon* **2014,** *71*, (0),

523 229-237.

524 42. Mkhoyan, K. A.; Contryman, A. W.; Silcox, J.; Stewart, D. A.; Eda, G.; Mattevi, C.; Miller, S.;

525 Chhowalla, M. *Nano Lett.* **2009,** *9*, (3), 1058-1063.

526 43. Auta, M.; Hameed, B. *Colloids Surf., B* **2013,** *105*, 199-206.

527 44. Mahmoodi, N. M.; Najafi, F.; Neshat, A. *Ind. Crop. Prod.* **2013,** *42*, 119-125.

528 45. Ramesha, G.; Kumara, A. V.; Muralidhara, H.; Sampath, S. *J colloid interf sci.* **2011**, *361*, 270.

Figure captions

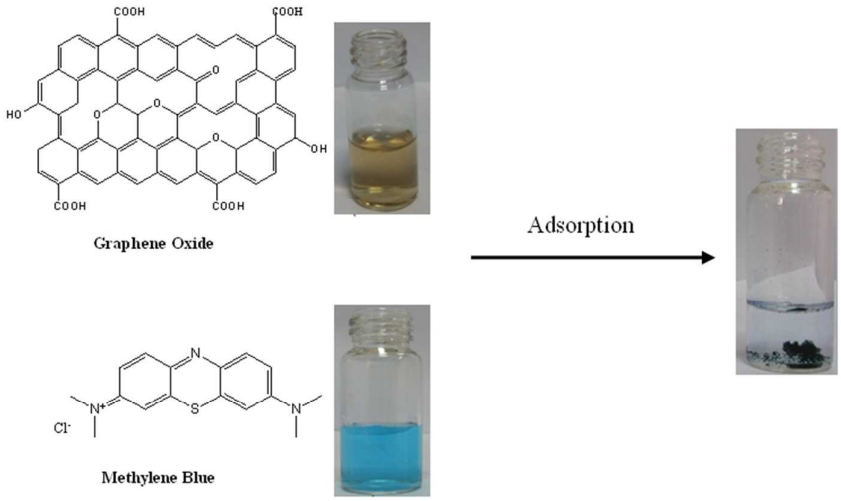

Fig 1. The schematic of the adsorption of MB onto GO. The total volume of 5 mL contains 25 μg MB (5 ppm) and 75 μg GO (15 ppm), with the presence of NaCl (5mM).

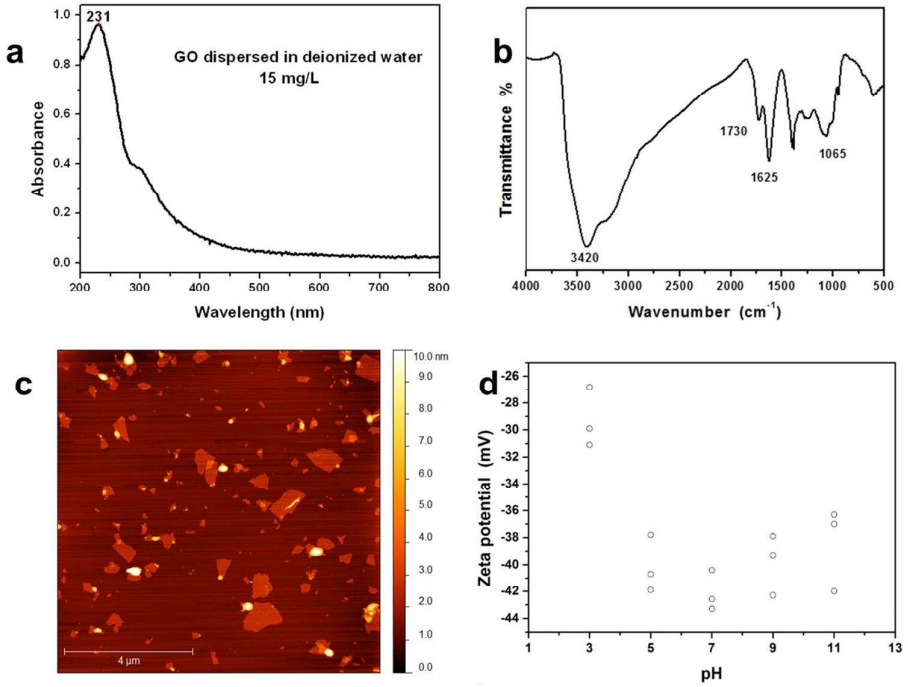

537

538 **Fig 2.** (a) UV-vis spectrum, (b) AFM image , (c) FTIR spectrum, and (d) Zeta potential of GO.

539

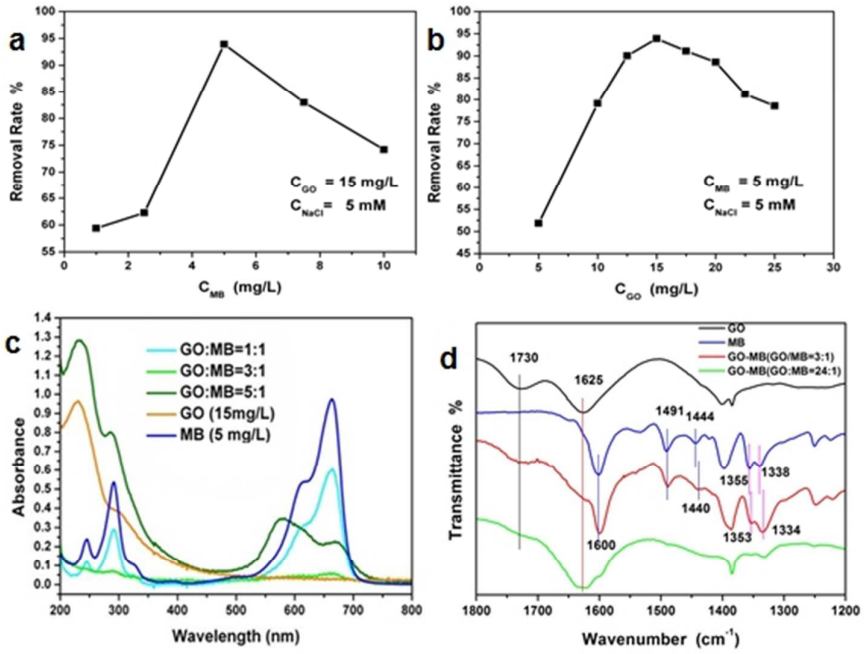

Fig 3. The MB removal performance as function of initial concentration of (a) MB and (b) GO; (c) UV-vis spectra of the solution with different ratios of GO to MB after dye removal, in the presence of 5mM NaCl; (d) FTIR spectra of GO/MB precipitates with a different ratio of GO and MB.

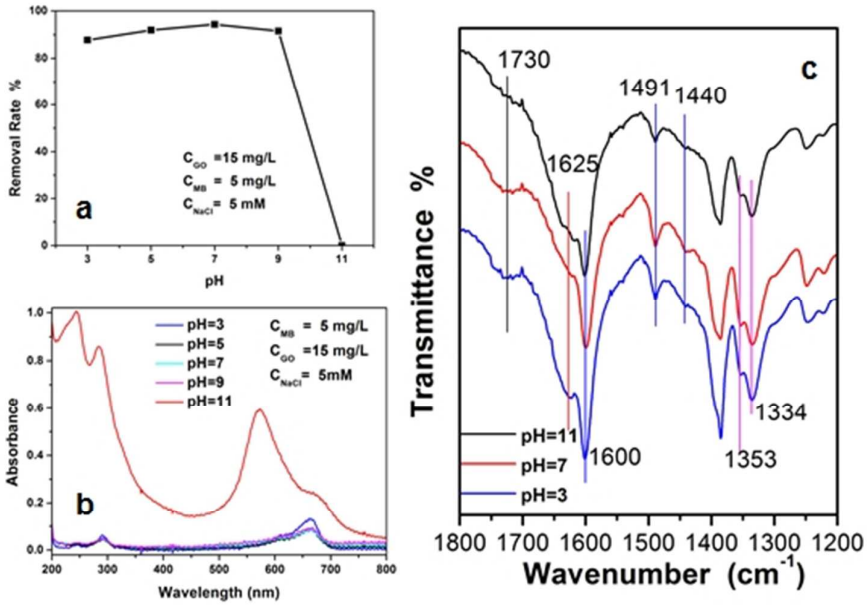

546

547

548 **Fig 4.** (a) The effect of solution pH on the dye removal efficiency; (b) UV-vis spectra of the
549 solutions after dye removal, (c) IR spectra of GO-MB residues formed at pH 3, 7, and 11,
550 respectively.

551

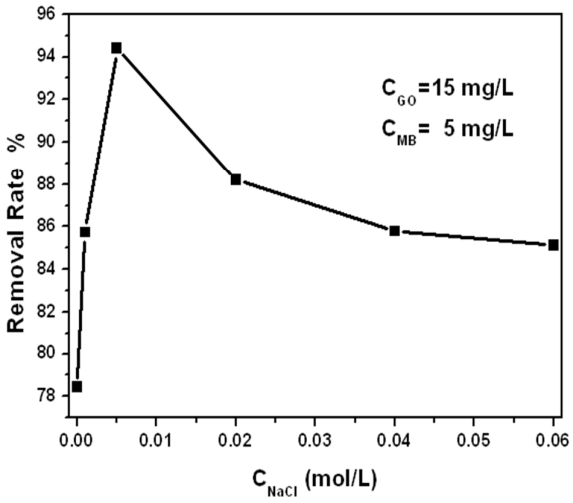

552

553

554 **Fig 5.** Effect of ionic strength on the dye removal efficiency.

555

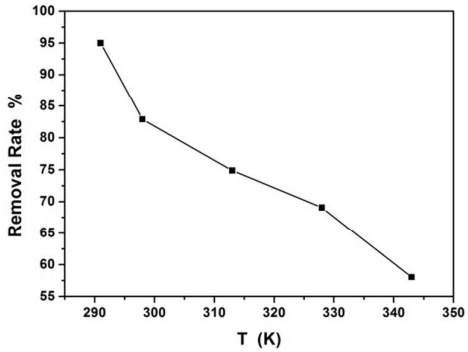

Fig 6. Effect of temperature on the dye removal efficiency.

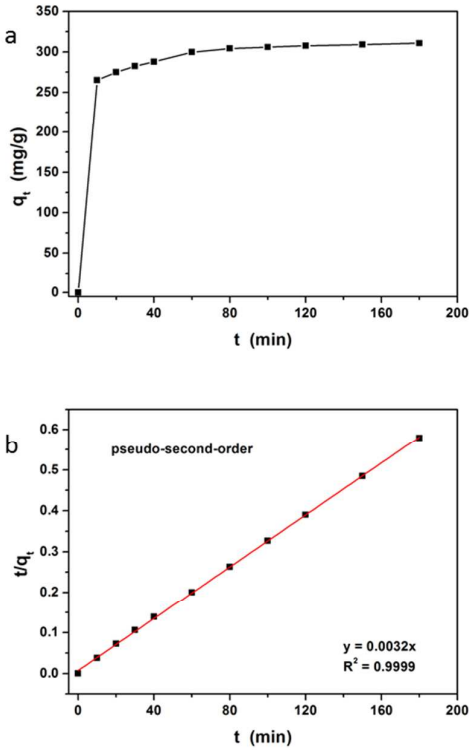

582

583 **Fig 7.** Effect of contact time on MB adsorbed onto GO (a) and the kinetic models:

584 pseudo-second-order model (b).

585

586 **Table 1.** Kinetic parameters for adsorption of MB onto GO.

587

Kinetic model		Kinetic parameters
Pseudo-first-order	$q_{e,calc}$	50.31
	k_1	0.0144
	R^2	0.9424
Pseudo-second-order	$q_{e,calc}$	312.5
	k_2	0.001138
	R^2	0.9999
Elovich	α	0.0588
	β	10^8
	R^2	0.9753
Intraparticle diffusion	k_i	7.5094
	L	241.19
	R^2	0.9987

588

589

590

591

592

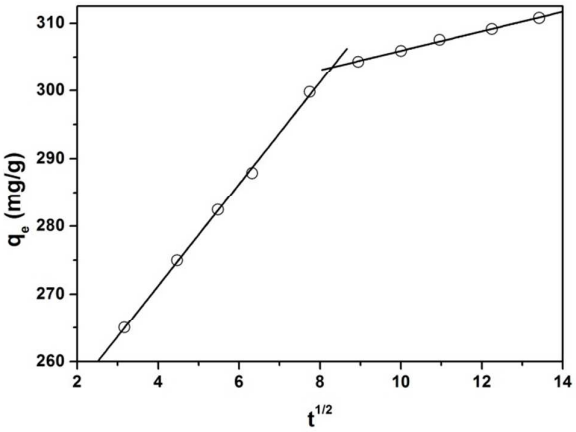

Fig 8. The intraparticle diffusion of MB by GO.

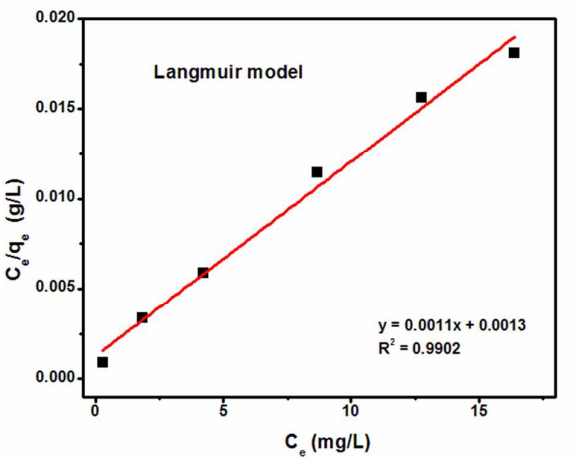

598
599
600 **Fig 9.** Langmuir isotherm for the adsorption of MB onto GO.
601
602

603 **Table 2.** The isotherm parameters for the adsorption of MB onto GO.

604

	isotherms					
parameters	Langmuir	Freundlich	Temkin	Redlich-Peterson	Sips	Dubinin-Radushkevich
K	0.846	453.6	33.25	7167.25	0.885	683.89
q_m	909.1				931.45	
n		3.99				
b			17.46		1.052	
α				15.801		
β				0.7494		$7*10^{-8}$
R^2	0.9902	0.978	0.9807	0.9875	0.9899	0.8573

605

606

607

608 **Table 3.** Comparison of adsorption capacity of various adsorbents for MB.

609

adsorbent	Adsorption capacity mg/g	Ref.
GO	48.76-598.8	[21]
GO	714	[26]
3D GO	397	[27]
GO	243.9	[34]
EGO	17.3	[44]
GO	909.1	This work

610

611

612

613

614

615

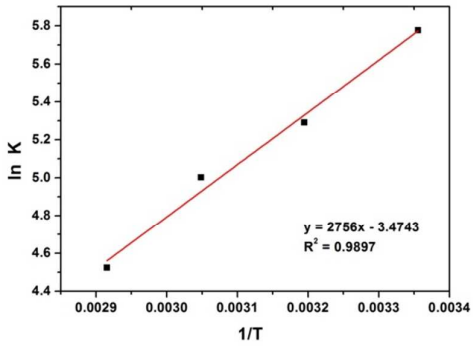

616

617 **Fig 10.** The plot of ln K vs. 1/T.

618

Table 4. Thermodynamic parameters for the adsorption of MB onto GO.

T (K)	ΔG^0 (kJ/mol)	ΔH^0 (kJ/mol)	ΔS^0 (J/mol K)
298	-14.31		
313	-13.77	-22.91	-28.88
328	-13.64		
343	-12.90		

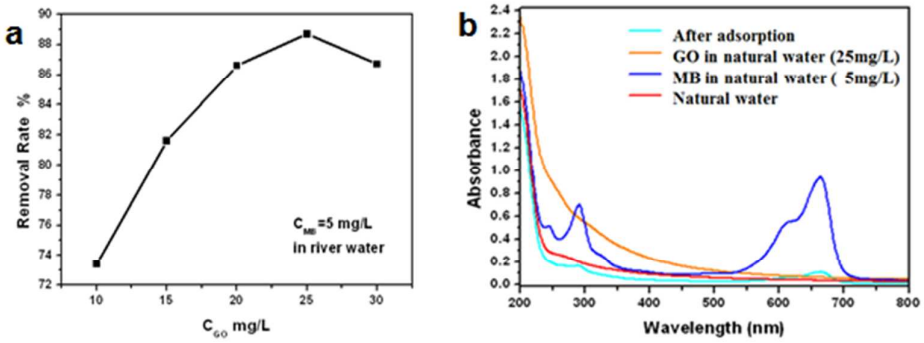

Fig 11. (a) MB removal rate in natural water at a fixed GO/MB ratio with a series of initial concentrations of GO. (b) UV-Vis spectra of the solution after dye removal process, 25 mg/mL of GO or 5 mg/mL of MB, in natural water.

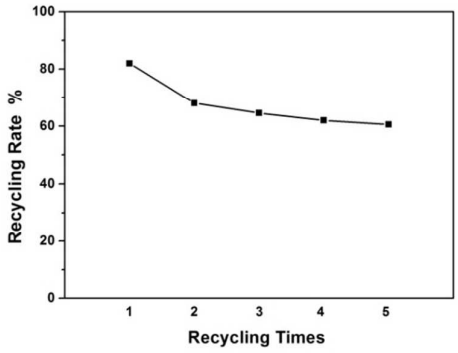

631

632

633 **Fig 12.** Recycling of MB for 5 times. 82% MB was recycled through ethanol extraction from the
634 GO/MB residues for the first recycling process. After 5 recycling process, recycling rate of MB
635 was still above 60%.

636

637 Table of Contents Entry

638

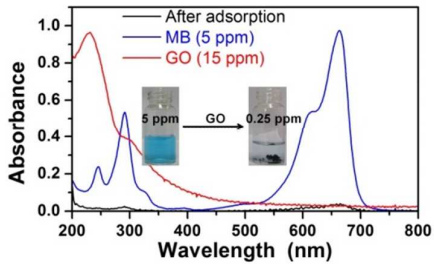

639

640 Methylene blue (several ppm) could be efficiently collected and easily recycled by graphene oxide

641 from solution via simple adsorption process.

642

643